Transversity and Polarization Reversal

Lingyan Zhu, UIUC

Polarized He3 Collaboration at JLab

Sep. 13, 2004

† HERMES and COMPASS Transverse Data †

† Collins Fragmentation Function †

† Polarization Reversal †

HERMES and COMPASS Transverse Data

- **Collins asymmetry from HERMES**

  Kinem:

  $0.023 < x < 0.4$,$0.2 < z < 0.7$,

  $W > \sqrt{10}\mathrm{GeV}$,$0.1 < y < 0.85$,$Q^2 > 1\mathrm{GeV}^2$

  $< x >= 0.09$,$< y >= 0.54$,$< Q^2 >= 2.41\mathrm{GeV}^2$, $< z >= 0.36$,

  $< P_{\pi\perp} >= 0.41\mathrm{GeV}$

  Results:

  $< \sin(\pi^+ + \phi_s) >_p^{\pi^+} = 0.021 \pm 0.007(\mathrm{stat.})$,

  $< \sin(\pi^+ + \phi_s) >_p^{\pi^-} = -0.038 \pm 0.008(\mathrm{stat.})$

- **Collins asymmetry from COMPASS**

  Kinem:

  $0.004? < x < 0.4?$,$z > 0.25$, $W > 5\mathrm{GeV}$,

  $0.1 < y < 0.9$,$Q^2 > 1\mathrm{GeV}^2$, $P_{\pi\perp} > 0.1\mathrm{GeV}$

  $< x >= 0.035$,$< y >= 0.33$,$< Q^2 >= 2.4\mathrm{GeV}^2$, $< z >= 0.45$,

  $< P_{\pi\perp} = \sqrt{0.3}\mathrm{GeV}$, $< W >= 9.4\mathrm{GeV}$

  Results:

  $A_d^{h+} \sim 0$, $A_d^{h-} \sim 0$

- **Definition comparison**

  HERMES weighted Collins moment:

  $2 < \sin(\pi^+ + \phi_s) >_{UT} = \frac{N_\uparrow - N_\downarrow}{N_\uparrow + N_\downarrow} \frac{1}{B/A \cdot |S_T|}$

  with $B/A = \frac{1-y}{y^2/2+(1-y)(1+\sigma_L/\sigma_T)/(1+2M_p x/(Ey))}$ and $|S_T|$ the proton polarization.

  COMPASS Collins Asymmetry:

  $A_{\mathrm{Coll}} = \frac{N_\uparrow - N_\downarrow}{N_\uparrow + N_\downarrow} \frac{1}{D_{NN} \cdot f \cdot P} = \frac{\sum_q e_q^2 \delta q H_{1\perp}^q}{\sum_q e_q^2 q D^q}$

  with $D_{\mathrm{NN}} = \frac{1-y}{y^2/2+(1-y)}$ and f the dilution factor, P target polarization.

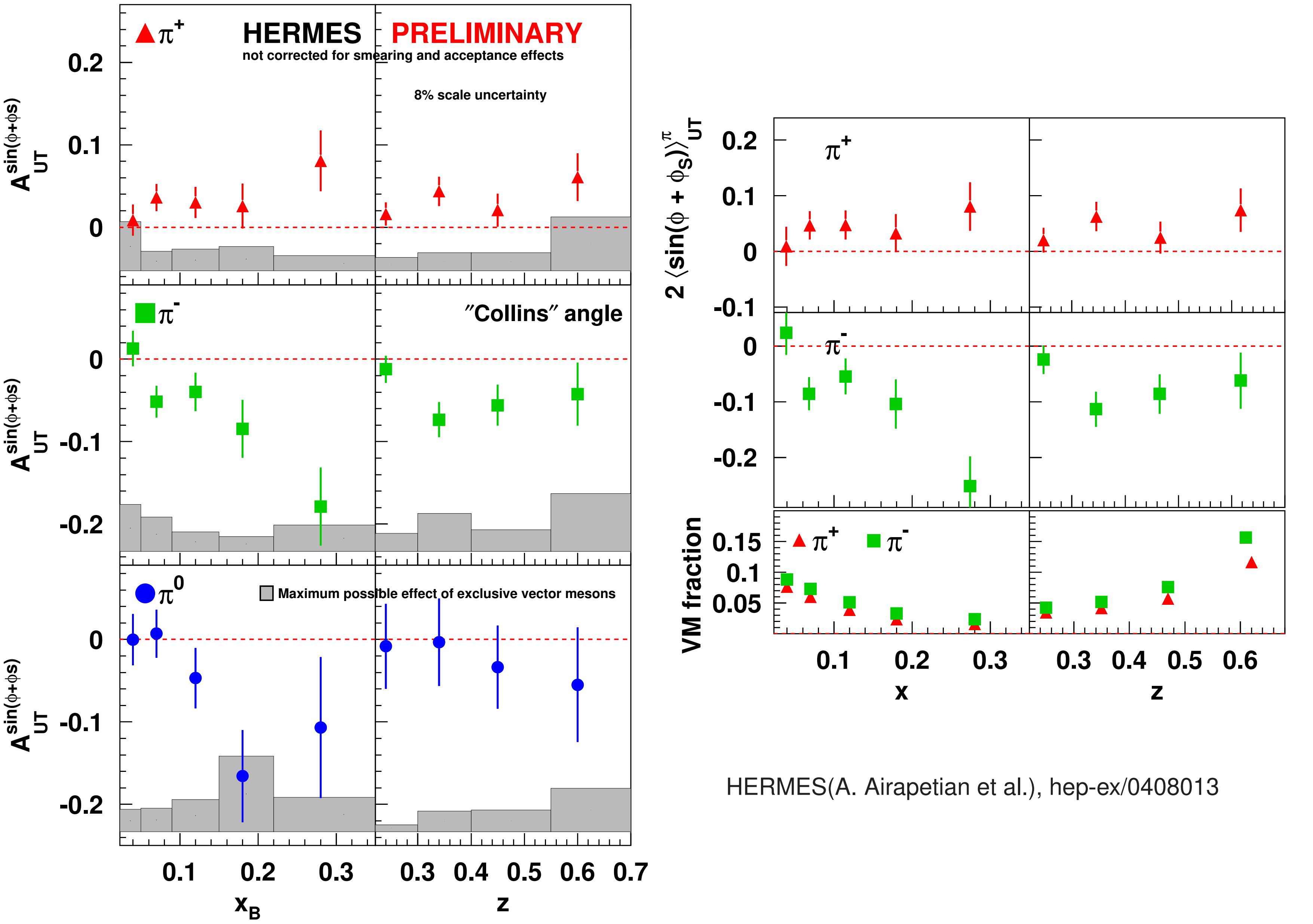

HERMES(A. Airapetian et al.), hep-ex/0408013

Collins-Asymmetrie (Deuteron)

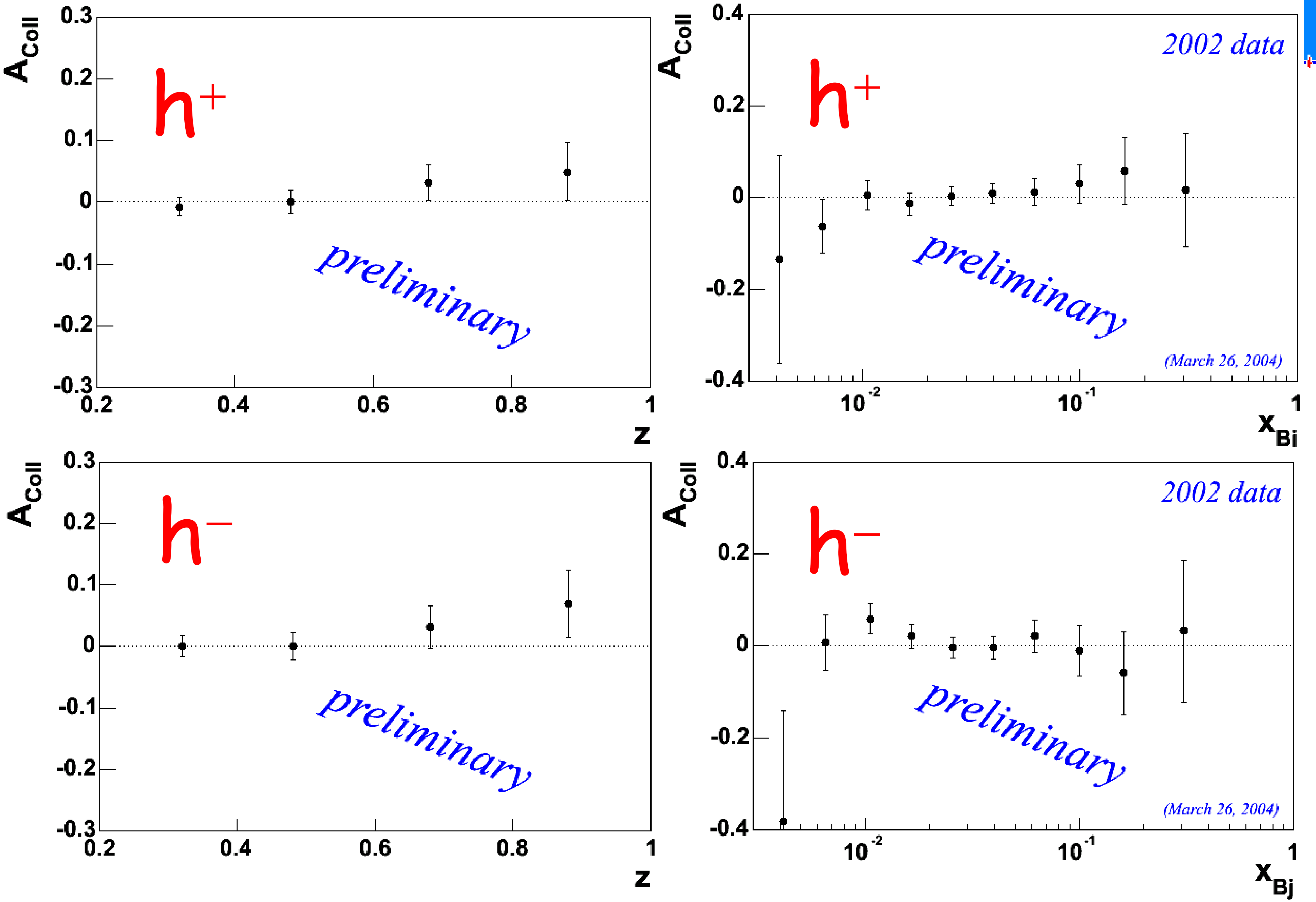

Implications of HERMES Transverse Data

- Data:$< \sin(\pi^+ + \phi_s) >^{\pi^+}_{UT} = 0.021 \pm 0.007(\text{stat.})$;
  $< \sin(\pi^+ + \phi_s) >^{\pi^-}_{UT} = -0.038 \pm 0.008(\text{stat.})$

- Assumptions:
  $H_{\text{fav}} \equiv H_{1\perp}^{u\to\pi^+} = H_{1\perp}^{d\to\pi^-} = H_{1\perp}^{\bar{u}\to\pi^-} = H_{1\perp}^{\bar{d}\to\pi^+}$
  $H_{\text{dis}} \equiv H_{1\perp}^{u\to\pi^-} = H_{1\perp}^{d\to\pi^+} = H_{1\perp}^{\bar{u}\to\pi^+} = H_{1\perp}^{\bar{d}\to\pi^-}$
  $D_{\text{dis}}/D_{\text{fav}} \sim 0.5$ at z=0.36 and $u \sim 2d$
  $\Rightarrow \frac{\sum_q e_q^2 q D^{q\to\pi^+}}{\sum_q e_q^2 q D^{q\to\pi^-}} \sim 1.7$

- Relations:
  $A_p^{\pi^+} \propto \frac{[4\delta u+\delta\bar{d}]H_{\text{fav}}+[\delta d+4\delta\bar{u}]H_{\text{dis}}}{[4u+\bar{d}]D_{\text{fav}}+[d+4\bar{u}]D_{\text{dis}}}$;
  $A_p^{\pi^-} \propto \frac{[4\delta u+\delta\bar{d}]H_{\text{dis}}+[\delta d+4\delta\bar{u}]H_{\text{fav}}}{[4u+\bar{d}]D_{\text{dis}}+[d+4\bar{u}]D_{\text{fav}}}$

- Implications:
  $\frac{\sum_q e_q^2 \delta q H^{q\to\pi^+}}{\sum_q e_q^2 \delta q H^{q\to\pi^-}} \sim 1.7 * \frac{0.021}{-0.038} = -0.94 \sim -1$
  $\Rightarrow [4\delta u + \delta d + 4\delta\bar{u} + \delta\bar{d}][H_{\text{fav}} + H_{\text{dis}}] \sim 0$
  $\Rightarrow H_{\text{fav}} = -H_{\text{dis}}$
  ($\delta d/\delta u = -0.93$ based on Wakamatsu *et al.*'s χQSM).

Implications of COMPASS Transverse Data

- Resutls: $A_d^{h+} \sim 0$; $A_d^{h-} \sim 0$
- Assumptions:

  $H_{\rm fav} \equiv H_{1\perp}^{u\to\pi^+} = H_{1\perp}^{d\to\pi^-} = H_{1\perp}^{\bar{u}\to\pi^-} = H_{1\perp}^{\bar{d}\to\pi^+}$

  $H_{\rm dis} \equiv H_{1\perp}^{u\to\pi^-} = H_{1\perp}^{d\to\pi^+} = H_{1\perp}^{\bar{u}\to\pi^+} = H_{1\perp}^{\bar{d}\to\pi^-}$

  $h^\pm \sim \pi^\pm$

- Implications:

  $\sum_q e_q^2 \delta q H_{1\perp}^{q\to\pi^+} =$

  $[4\delta u + 4\delta d + \delta\bar{u} + \delta\bar{d}] H_{\rm fav} + [\delta u + \delta d + 4\delta\bar{u} + 4\delta\bar{d}] H_{\rm dis} \sim 0$

  $\sum_q e_q^2 \delta q H_{1\perp}^{q\to\pi^-} =$

  $[4\delta u + 4\delta d + \delta\bar{u} + \delta\bar{d}] H_{\rm dis} + [\delta u + \delta d + 4\delta\bar{u} + 4\delta\bar{d}] H_{\rm fav} \sim 0$

  $\Rightarrow |H_{\rm dis}| \sim |H_{\rm fav}|, |4\delta u + 4\delta d + \delta\bar{u} + \delta\bar{d}| \sim |\delta u + \delta d + 4\delta\bar{u} + 4\delta\bar{d}|$

  if $H_{\rm dis}, H_{\rm fav}, [4\delta u + 4\delta d + \delta\bar{u} + \delta\bar{d}], [\delta u + \delta d + 4\delta\bar{u} + 4\delta\bar{d}] \neq 0$

  $\Rightarrow \delta u + \delta d = 0$ if sea quark contribution $\delta\bar{u}$ and $\delta\bar{d}$ can be ignored and $H_{\rm dis}, H_{\rm fav} \neq 0$.

  χQSM: $\delta d/\delta u = -0.93$ (Wakamatsu)

Projection for He3 target

- Collins part:
  $\sum_q^{He3} e_q^2 \delta q H^{q\to\pi} = \sum_q^{p} e_q^2 \delta q H^{q\to\pi} + \sum_q^{d} e_q^2 \delta q H^{q\to\pi} \sim \sum_q^{p} e_q^2 \delta q H^{q\to\pi}$

- Unpolarized part:
  $\sum_q^{He3} e_q^2 q D^{q\to\pi^+} = \sum_q^{p} e_q^2 q D^{q\to\pi^+} + \sum_q^{d} e_q^2 q D^{q\to\pi^+} \sim 2.5 \sum_q^{p} e_q^2 \delta q H^{q\to\pi^+}$
  $\sum_q^{He3} e_q^2 q D^{q\to\pi^-} = \sum_q^{p} e_q^2 q D^{q\to\pi^-} + \sum_q^{d} q e_q^2 D^{q\to\pi^-} \sim 3 \sum_q^{p} e_q^2 \delta q H^{q\to\pi^-}$

- Projections:
  $A_{He3}^{\pi^+} \sim 0.4 A_p^{\pi^+}$
  $A_{He3}^{\pi^-} \sim 0.3 A_p^{\pi^-}$

Implications of HERMES π^0 Data

- Data: $< \sin(\pi^+ + \phi_s) >_{UT}^{\pi^0} \sim < \sin(\pi^+ + \phi_s) >_{UT}^{\pi^-}$?

- Relations:

$$A_p^{\pi^0} \propto \frac{[4\delta u + \delta\bar{d} + \delta d + 4\delta\bar{u}]\cdot[H_{\rm fav} + H_{\rm dis}]/2}{[4u + \bar{d} + d + 4\bar{u}]\cdot[D_{\rm fav} + D_{\rm dis}]/2};$$

$$A_p^{\pi^-} \propto \frac{[4\delta u + \delta\bar{d}]H_{\rm dis} + [\delta d + 4\delta\bar{u}]H_{\rm fav}}{[4u + \bar{d}]D_{\rm dis} + [d + 4\bar{u}]D_{\rm fav}}$$

- Assumptions:

$$H_{\rm fav} \equiv H_{1\perp}^{u\to\pi^+} = H_{1\perp}^{d\to\pi^-} = H_{1\perp}^{\bar{u}\to\pi^-} = H_{1\perp}^{\bar{d}\to\pi^+}$$

$$H_{\rm dis} \equiv H_{1\perp}^{u\to\pi^-} = H_{1\perp}^{d\to\pi^+} = H_{1\perp}^{\bar{u}\to\pi^+} = H_{1\perp}^{\bar{d}\to\pi^-}$$

$D_{\rm dis}/D_{\rm fav} \sim 0.5$ at z=0.36 and $u \sim 2d$

$$\Rightarrow \frac{\sum_q e_q^2 q D^{q\to\pi^0}}{\sum_q e_q^2 q D^{q\to\pi^-}} = 1.3 \sim 1$$

- Implications:

$\frac{\sum_q e_q^2 \delta q H^{q\to\pi^0}}{\sum_q e_q^2 \delta q H^{q\to\pi^-}} \sim 1$ and $\sum_q e_q^2 \delta q H^{q\to\pi^0} < 0$

$\Rightarrow H_{\rm fav} \neq -H_{\rm dis}$ and $[4\delta u + \delta d + 4\delta\bar{u} + \delta\bar{d}] \neq 0$

$$\Rightarrow \sum_q e_q^2 \delta q H^{q\to\pi^+} = 2\sum_q e_q^2 \delta q H^{q\to\pi^0} - \sum_q e_q^2 \delta q H^{q\to\pi^-} < 0$$

Inconsistent with transversity measurements for π^+.

Size of Collins Function

• DELPHI

Efremov et al., hep-ph/9812522

Transverse q, $\overline{q}$ polarization small but ANTI-CORRELATED (@ $\sim$ 50 % level)

$$\left|\frac{H_1^\perp}{D_1}\right| = 6.3 \pm 1.7\,\%$$

• HERMES / SMC

Efremov et al., hep-ph/0108213

Fit experimental data for $H_1^\perp$, taking $h_1(x)$ from Chiral Quark Soliton Model (χQSM)

$$\left|\frac{H_1^\perp}{D_1}\right| = \begin{cases} 6.1 \pm 0.9 \pm 0.8\% \ \text{(HERMES)} \\ 10 \pm 5\% \ \text{(SMC)} \end{cases}$$

• E704

Boglione & Mulders, PRD 60 (1999) 054007

Fit experimental data, assuming ONLY Collins effect contributes

$$\left|\frac{H_1^\perp}{D_1}\right| = 7.6\%$$

There seems to be general agreement

(although results depend on z-range over which averaging performed)

What about the Sivers Function?

- Note: fit to E704 assuming ONLY Sivers effect contributes:

$$\left|\frac{f_{1T}^\perp}{f_1}\right| = 8.3\% \quad \left(\text{“max” size}\right)$$

- MORE DATA NEEDED ... e.g. DIS w transverse target

$$A_{UT} \text{ has term } \sim f_{1T}^\perp\, D_1\, \sin(\phi_h^l + \phi_s^l)$$

Collins Fragmentation Function

I) Two-Jet-method

- $e^+e^- \rightarrow \pi^+_{jet1}\pi^-_{jet2}X$
- Reaction plane defined with beam (z-axis) and jet axis
- Hadron plane defined with π and jet axis on each side:
  - ϕ_i : angle between the planes

$A \propto H_1^{\perp}(z_1)H_1^{\perp}(z_2)\cos(\phi_1+\phi_2)$

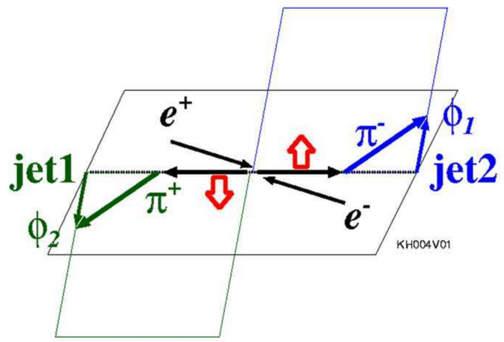

II) Two-hadron-method

- Can analyze with/without using jet axis

$A \propto H_1^{\perp}(z_1)H_1^{\perp}(z_2)\cos(2\phi)$

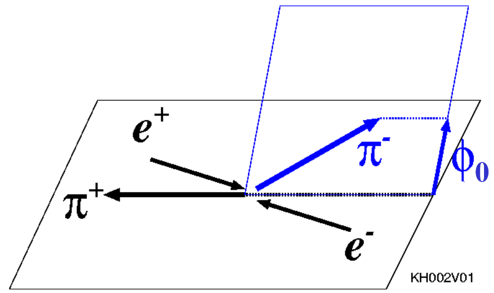

Polarization Reversal

- Goal:

  flip the laser beam frequently (on the level of minutes) with $\bar{\lambda} = 795$ nm, $D \sim 2$ inches.

- Possible solutions:

  – motorized transporter+half waveplate

    Speed is a big constrain.

  – motorized rotary stage+quarter waveplate

    Standa 8MR180-2: speed=1 turn/min or greater; 0.01 deg angular resolution.

  – liquid crystal waveplate

    Meadowlark liquid crystal variable retarder: $D = 1, 2, 3$ in; 0(+30 nm) to 1/2 wave with (without) compensator.

- Current Status:

  Wait for the test on the liquid crystal waveplate.

  (already ordered by Sirish for Compton)

These products all use nematic liquid crystal materials to electrically control polarization. Meadowlark Optics' standard liquid crystal products provide tunable retardation by changing the effective birefringence of the material with applied voltage, thus altering the transmitted light to some elliptical polarization form.

Our precision Liquid Crystal Variable Retarders require unique fabrication and assembly steps. We construct these retarders using optically flat fused silica windows coated with our transparent conductive indium tin oxide (ITO). Our ITO coating is specially designed for maximum transmission from 450-1800 nm. A thin dielectric layer is applied over the ITO and gently rubbed, to provide for liquid crystal molecular alignment. Two windows are then carefully aligned and spaced a few microns apart. The cavity is filled with birefringent nematic liquid crystal material. Electrical contacts are attached and the device is environmentally sealed. We carefully place the Liquid Crystal Variable Retarder in an anodized aluminum housing such that the fast and slow axes are both at 45° relative to a convenient mounting hole.

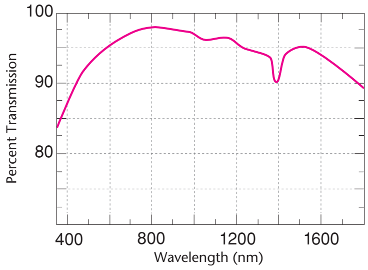

Fig. 4-5 Typical LC Transmission

Anisotropic nematic liquid crystal molecules form uniaxial birefringent layers in the liquid crystal cell. An essential feature of nematic material is that, on average, molecules are aligned with their long axes parallel, but with their centers randomly distributed as shown in figure 4-6(a). With no voltage applied, the liquid crystal molecules lie parallel to the glass substrates and maximum retardation is achieved.

When voltage is applied, liquid crystal molecules begin to tip perpendicular to the fused silica windows as shown in figure 4-6(b). As voltage increases, molecules tip further causing a reduction in the effective birefringence and hence, retardance. Molecules at the surface, however, are unable to rotate freely because they are pinned at the alignment layer. This surface pinning causes a residual retardance of ~30 nm even at high voltage (20 volts).

We achieve zero (or any custom) retardance with a subtractive fixed polymer retarder, called a compensator, attached to the liquid crystal cell. Negative retardance values are sometimes preferred, for example, when converting between right- and left-circularly polarized states. Figure 4-7 illustrates retardance as a function of voltage for a typical Liquid Crystal Variable Retarder with and without an attached compensator. Placing a compensated Liquid Crystal Variable Retarder between two high extinction polarizers creates an excellent optical attenuator, with convenient electronic control.

As with any birefringent material, retardance is dependent upon thickness and birefringence. Liquid crystal material birefringence depends on operating wavelength, drive voltage, and temperature. The overall retardance of a liquid crystal cell decreases with increasing temperature (approximately -0.4% per °C).

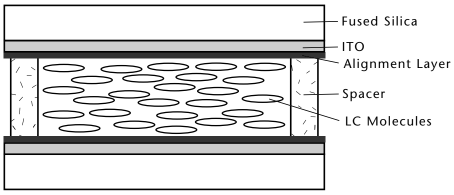

(a) Maximum Retardance (V = 0)

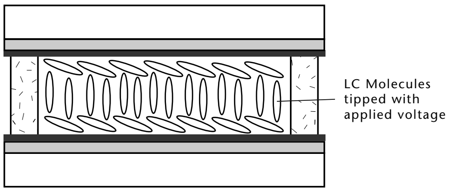

(b) Minimum Retardance (V >> 0)

Fig. 4-6 Liquid Crystal Variable Retarder construction showing molecular alignment (a) without and (b) with applied voltage (drawing not to scale)

Liquid Crystal Variable Retarders

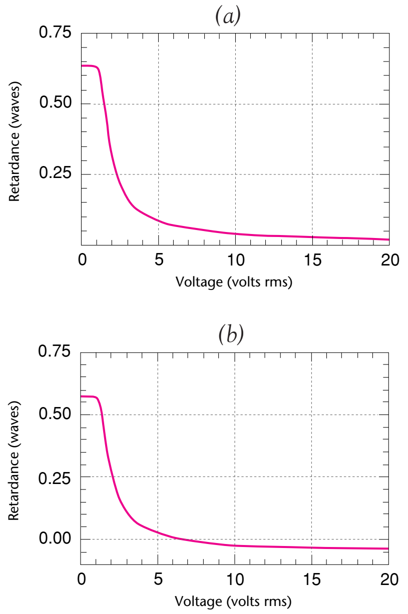

Fig. 4-7 Liquid Crystal Variable Retarder performance at 632.8 nm, 21 °C (a) without compensator, and (b) with compensator

APPLICATION NOTE

Response Time

Liquid Crystal Variable Retarder response time depends on several parameters, including layer thickness, viscosity, temperature, variations in drive voltage, and surface treatment. Liquid crystal response time is proportional to the square of the layer thickness and therefore, the square of the total retardance.

Response time also depends upon direction of the retardance change. If the retardance increases, response time is determined solely by mechanical relaxation of the molecules. If retardance decreases in value, response time is much faster due to the increased electric field across the liquid crystal layer. Typical response time for our standard visible Liquid Crystal Variable Retarder is shown in figure 4-8. It takes about 5 ms to switch from one-half to zero waves (low to high voltage) and about 20 ms to switch from zero to one-half wave (high to low voltage).

Response time improves by using custom materials with high birefringence and a thinner liquid crystal layer. At higher temperature, material viscosity decreases, also contributing to a faster response.

Another technique involves the Transient Nematic Effect (TNE) to improve response times. With this drive method, a high voltage spike is applied to accelerate the molecular alignment parallel to the applied field. Voltage is then reduced to achieve the desired retardance. When switching from low to high retardance all voltage is momentarily removed to allow the liquid crystal molecules to undergo natural relaxation. Response time achieved with the transient nematic effect is also shown in figure 4-8. Our programmable D3040 Controller described on page 45 can provide the necessary TNE voltage profiles.

Our standard Liquid Crystal Variable Retarders provide a minimum retardance range of ~30 nm to at least half-wave at the specified wavelength. With an attached compensator, retardance is guaranteed from zero to at least half-wave at the specified wavelength. Custom retardance ranges (up to a few waves) and custom compensators are available. Contact our Sales Department to discuss your requirements.

Each Liquid Crystal Variable Retarder is supplied with retardance versus voltage performance data for your specified wavelength. A coaxial cable with BNC connector is provided for easy attachment to an electronic controller.

Liquid crystal devices should be electrically driven with an AC waveform with **no DC component** to prevent

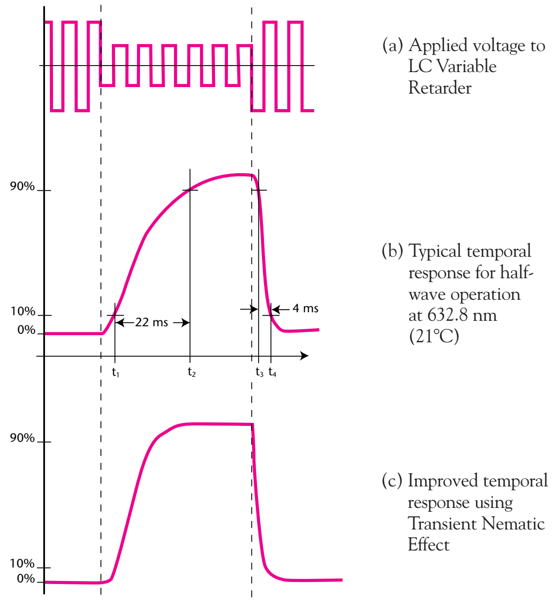

Fig. 4-8 Temporal response of LC Variable Retarder

PROBLEM *"The temporal response of a liquid-crystal device seems very complicated. Where can I find some clarification?"*

SOLUTION Click here to see our application note on temporal response of liquid crystal devices.